7576 *Inorg. Chem.* **2009**, *48*, 7576–7584
DOI: 10.1021/ic900699h

Inorganic Chemistry
Article

Surfactant-Assisted Hydrothermal Synthesis of Eu^{3+}-Doped White Light Hydroxyl Sodium Yttrium Tungstate Microspheres and Their Conversion to $NaY(WO_4)_2$

Fang Lei,[†] Bing Yan,*[,†] Hao Hong Chen,[‡] and Jing Tai Zhao[‡]

[†]*Department of Chemistry, Tongji University, Siping Road 1239, Shanghai 200092, China, and*
[‡]*Key Laboratory of Transparent Opto-functional Inorganic Materials, Shanghai Institute of Ceramics, Chinese Academy of Sciences, Dingxi Road 1295, Shanghai 200050, China*

Received January 20, 2009

In this work, large-scale three-dimensional "flake-ball" microarchitectures of Eu^{3+} doped white light hydroxyl sodium yttrium tungstate were prepared by the well-known hydrothermal approach at 180 °C for 48 h in the presence of triblock-copolymer poly(ethylene glycol)-block-poly(propylene glycol)-block-poly(ethylene glycol) (P123). $NaY(WO_4)_2:Eu^{3+}$ phosphor was formed by annealing the hydrothermal product at ~630 °C for 2 h. A time-dependent microstructure evolution study was performed under hydrothermal reaction. The evolution process is the self-assembly process of P123, and the effects of other reaction parameters, such as influence of the concentration of P123 on morphology, and the influence of temperature on PL. The mechanism by which the "flake-ball" particles are formed is discussed in detail. The PL spectra of Eu^{3+}-doped hydroxyl sodium yttrium tungstate phosphor contain two parts: the broad blue-green band and the $^5D_0 \rightarrow {}^7F_J$ ($J = 1$, and 2) characteristic transition of Eu^{3+}. This approach provides a facile route for the production of high-quality hydroxyl sodium yttrium tungstate microstructures with an interesting optical property.

1. Introduction

Double alkaline rare-earth molybdates and tungstates with the formula of $ARE(MO_4)_2$ (A = Na, K, RE = Y, La, Gd, Lu, and M = Mo, W) form a wide variety of inorganic compounds having tetragonal and monoclinic symmetries that have attracted great interest in recent years.[1−6] Their structure diversity provides these crystals with numerous physical and chemical properties for the possibility of doping with rare earth ions without substantial fluorescence quenching, in addition to the well-known laser hosts. The $ARE(MO_4)_2$ family compounds were reported mostly on the single crystals to be used as laser crystal materials for a long period of time.[7−13] Tungstate with a sheelite-type structure has been of practical interest because of its attractive luminescence property with the promising applications in photoluminescence (PL), optical fibers, and scintillators.[14] As one compound of the family, $NaY(WO_4)_2$ has a tetragonal symmetry with the structure of scheelite $CaWO_4$ (W^{6+} is coordinated by four oxygen atoms in a tetrahedral site and Y^{3+}/Na^+ site is eight coordinated). It has been demonstrated to be a promising host lattice for lasing ions.[15,16]

While as novel phosphors, the $ARE(MO_4)_2$ family and their precursors have received little attention. Herein, we present the red Eu^{3+} doped $NaY(WO_4)_2$ phosphor and its morphology-controlled precursor hydroxyl sodium yttrium tungstate white light phosphor first. There have been great many studies on the preparation of hierarchical architectures

*To whom correspondence should be addressed. E-mail: byan@tongji.edu.cn. Phone: +86-21-65984663. Fax: +86-21-65982287.

(1) Wang, F.; Fan, X. P.; Pi, D. B.; Wang, Z. Y.; Wang, M. Q. *J. Solid State Chem.* **2005**, *178*, 825.
(2) Macalik, L. *J. Alloys Compd.* **2002**, *341*, 226.
(3) Alvarez-Vega, M.; Rodríguez-Carvajal, J.; Reyes-Cárdenas, J. G.; Fuentes, A. F.; Amador, U. *Chem. Mater.* **2001**, *13*, 3871.
(4) Kasprowicz, D.; Mielcarek, S.; Trzaskowska, A.; Majchrowski, A.; Michalski, E.; Drozdowski, M. *Cryst. Res. Technol.* **2007**, *42*, 1370.
(5) Petrov, V.; Pujol, M. C.; Mateos, X.; Silvestre, O.; Rivier, S.; Aguilo, M.; Sole, R. M.; Liu, J. H.; Griebner, U.; Dia, F. *Laser Photonics Rev.* **2007**, *1*, 179.
(6) Wang, K. P.; Zhang, J. X.; Wang, J. Y.; Yu, W. T.; Zhang, H. J.; Wang, Z. P. *J. Appl. Crystallogr.* **2005**, *38*, 975.
(7) Kato, A.; Oishi, S.; Shishido, T.; Yamazaki, M.; Lida, S. *J. Phys. Chem. Solids* **2005**, *66*, 2079.
(8) Kim, T.; Kang, S. *J. Lumin.* **2007**, *122−123*, 964.
(9) Cheng, Z. X.; Yi, X. J.; Han, J. R.; Chen, H. C.; Wang, X. L.; Liu, H. K.; Dou, S. X.; Song, F.; Guo, H. C. *Cryst. Res. Technol.* **2002**, *37*, 1318.
(10) Han, X. M.; García-Cortés, A.; Serrano, M. D.; Zaldo, C.; Cascales, C. *Chem. Mater.* **2007**, *19*, 3002.
(11) Jayaraman, A.; Sharma, S. K.; Wang, S. Y. *J. Raman Spectrosc.* **1998**, *29*, 305.
(12) Pujol, M. C.; Rico, M.; Zaldo, C.; Sole, R.; Nikolov, V.; Solans, X.; Aguilo, M.; Diza, F. *Appl. Phys. B: Lasers Opt.* **1999**, *68*, 187.
(13) Musset, O.; Boquillon, J. P. *Appl. Phys. B: Lasers Opt.* **1997**, *65*, 13.
(14) Jin, Y.; Zhang, J. H.; Lu, S. Z.; Zhao, H. F.; Zhang, X.; Wang, X. J. *J. Phys. Chem. C* **2008**, *112*, 5860.
(15) Cheng, Z. X.; Zhang, Sh. J.; Han, J. R.; Chen, H. C.; Lu, Q. M.; Guo, H. C. *Cryst. Res. Technol.* **2001**, *36*, 449.
(16) Fan, J. D.; Zhang, H. J.; Yu, W. T.; Yu, H. H.; Wang, J. Y.; Jiang, M. H. *J. Appl. Crystallogr.* **2008**, *41*, 584.

 Published on Web 07/10/2009

by assembling nanosized crystals with anisotropic structures.[17−20] The architecture is expected to exhibit characteristic physical and chemical properties depending on the size, morphology, alignment and dimensionality. Using block copolymers to control the nucleation, growth, and alignment of inorganic particles has been widely accepted in preparing morphogenesis of inorganic materials.[21−23] The precursor hydroxyl sodium yttrium tungstate obtained by facile hydrothermal reaction using triblock-copolymer poly(ethylene oxide)-poly (propylene oxide)-poly(ethylene oxide) (P123) as the structure-directing agent possesses the "flake-ball" microstructure and excellent PL properties. Under the UV excitation, the precursor doped with a certain amount of Eu^{3+} can emit white-light PL. The white light PL spectra is composed of two parts: the blue-green light range from 300 to 600 nm is related to the charge transfer (CT) from O→W of tungstate and the red light of the characteristic transition ($^5D_0 \rightarrow {}^7F_1$ and $^5D_0 \rightarrow {}^7F_2$) of Eu^{3+}. Huang et al. have reported the white-light phosphor yttrium tungstate-chloride xerogel without activator ions, its white light was identified as two emission bands of 300−400 nm (CTB of tungstate group) and 400−650 nm (oxygen defects in the structure).[24] It is widely accepted that some tungstate compounds have intrinsic luminescence related to the CT transition from O to W of tungstate. When doped with activator ions, some tungstates possess combined emission properties. Neeraj et al. had investigated novel red phosphors $NaM(WO_4)_{2-x}(MoO_4)_x$:Eu^{3+} (M = Gd, Y, Bi), which have potential application as red phosphors for white lighting devices utilizing the GaN-based excitation in the near UV.[25] Fan et al. reported the luminescence behavior of rare-earth-doped $NaLa(WO_4)_2$ powders, which was synthesized by the hydrothermal method.[1] Jing et al. also investigated the influence of fluoride on f-f transitions of Eu^{3+} in $LiEuM_2O_8$ (M = Mo, W).[26]

Nowadays, rare earth ions doped inorganic phosphors have extensive applications in almost any high-resolution display devices and lights, such as cathode ray tubes (CRTs), plasma displays panels (PDPs), field emission displays (FEDs), fluorescent lamps, and so on.[27−31] Eu^{3+} doped nano- and micro- crystals have been widely applied as red phosphors for color displays and fluorescent lamps in terms of their high emission intensities and well predictable emission wavelengths from the intraconfigurational f-f transitions of Eu^{3+} ions.[32−34]

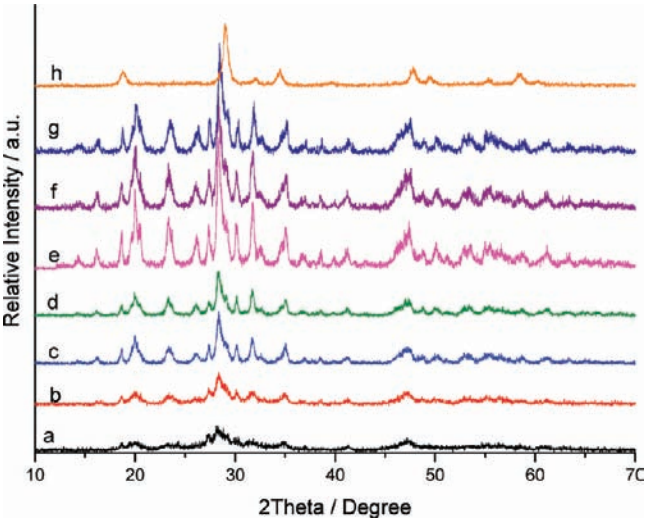

Figure 1. Time dependent XRD patterns of the product synthesized by hydrothermal method at different time intervals (a) 1 h, (b) 3 h, (c) 6 h, (d) 12 h, (e) 24 h, (f) 48 h, (g) 72 h, and (h) the hydrothermal product obtained at 180 °C for 48 h with annealing at 630 °C for 2 h.

In this paper, we present the hydrothermal route for the synthesis of uniform spherical hydroxyl sodium yttrium tungstate precursor assembled with single-crystal nanoflakes by adjusting the hydrothermal conditions, and $NaY(WO_4)_2$ crystals were prepared by annealing hydroxyl sodium yttrium tungstate at ∼630 °C for 2 h. The mechanism of the formation of a uniform-sized spherical precursor was examined. Room temperature PL spectra of the as-synthesized hydroxyl sodium yttrium tungstate crystals revealed that the optical properties could be modulated by adjusting the doping concentration of Eu^{3+}.

2. Experimental Section

2.1. Chemicals. Europium oxide (Eu_2O_3 (99.99%)), yttrium oxide (Y_2O_3 (99.99%)), sodium tungstate ($Na_2WO_4 \cdot H_2O$ (AR)), HNO_3, and triblock copolymer Pluronic P123 ($EO_{20}PO_{70}EO_{20}$, Aldrich) were used as the raw materials without further purification. The structural composition of this polymer is HO-$(C_2H_4O)_{20}(C_3H_6O)_{70}(C_2H_4O)_{20}H$, it has a number-average molecular weight of 5800 g/mol.

2.2. Synthesis Procedures. In a representative synthesis route, the given amount of rare-earth nitrate (Y^{3+} and Eu^{3+}) were prepared by dissolving corresponding Eu_2O_3−Y_2O_3 ($(2 - x)$ mmol Y^{3+} and x mmol Eu^{3+} (x = 0, 0.02, 0.04, 0.06, and 0.08), the molar ratios of Eu^{3+}/Y^{3+} vary from 0.01 to 0.05) in HNO_3, and excess HNO_3 was removed by evaporation. The solution A was prepared by dissolving the obtained rare earth nitrate (containing Y^{3+} and Eu^{3+}) in 5 mL of deionized water, solution B was prepared by dissolving $Na_2WO_4 \cdot 2H_2O$ (the molar ratio of RE/W is 2: 1) and ∼0. 050 g of poly(ethylene glycol)-block-poly(propylene glycol)-block-poly(ethylene glycol) (P123) in 5 mL of heated deionized water (∼75 °C) with initial pH 8.0

(17) Amano, F.; Nogami, K.; Abe, R.; Ohtani, B. *J. Phys. Chem. C* **2008**, *112*, 9320.
(18) Shi, H. T.; Qi, L. M.; Ma, J. M.; Cheng, H. M. *J. Am. Chem. Soc.* **2003**, *125*, 3450.
(19) Cao, A. M.; Hu, J. S.; Liang, H. P.; Song, W. G.; Wan, L. J.; He, X. L.; Gao, X. G.; Xia, S. H. *J. Phys. Chem. B* **2006**, *110*, 15858.
(20) Sounart, T. L.; Liu, J.; Voigt, J. A.; Hsu, J. W. P.; Spoerke, E. D.; Tian, Z.; Jiang, Y. B. *Adv. Funct. Mater.* **2006**, *16*, 335.
(21) Qi, L. M.; Li, J.; Ma, J. M. *Adv. Mater.* **2002**, *14*, 300.
(22) Cölfen, H.; Qi, L. M.; Mastai, Y.; Börger, L. *Cryst. Growth Des.* **2002**, *2*, 191.
(23) Zhang, D. B.; Qi, L. M.; Ma, J. M.; Cheng, H. M. *Chem. Mater.* **2002**, *14*, 2450.
(24) Huang, J. P.; Luo, H. S.; Yu, X. B.; Li, Y. K.; Zou, W. L. *J. Lumin.* **2008**, *128*, 589.
(25) Neeraj, S.; Kijima, N.; Cheetham, A. K. *Chem. Phys. Lett.* **2004**, *387*, 2.
(26) Wang, J. G.; Jing, X. P.; Yan, Ch. H.; Lin, J. H.; Liao, F. H. *J. Lumin.* **2006**, *121*, 57.
(27) Byeon, S. H.; Ko, M. G.; Park, J. C.; Kim, D. K. *Chem. Mater.* **2002**, *14*, 603.
(28) Yu, M.; Lin, J.; Wang, Z.; Fu, J.; Wang, S.; Zhang, H. J.; Han, Y. C. *Chem. Mater.* **2002**, *14*, 2224.
(29) Jennifer, A.; Nelson, E. L. B.; Michael, J. W. *Chem. Mater.* **2003**, *15*, 688.
(30) Wu, C. C.; Chen, K. B.; Lee, C. S.; Chen, T. M.; Cheng, B. M. *Chem. Mater.* **2007**, *19*, 3278.
(31) Lai, H.; Bao, A.; Yang, Y. M.; Tao, Y. C.; Yang, H.; Zhang, Y.; Han, L. L. *J. Phys. Chem. C* **2008**, *112*, 282.
(32) Fujihara, S.; Tokumo, K. *Chem. Mater.* **2005**, *17*, 5587.
(33) Nedelec, J. M.; Avignant, D.; Mahiou, R. *Chem. Mater.* **2002**, *14*, 651.
(34) Ptacek, P.; Schäfer, H.; Kömpe, K.; Haase, M. *Adv. Funct. Mater.* **2007**, *17*, 3843.

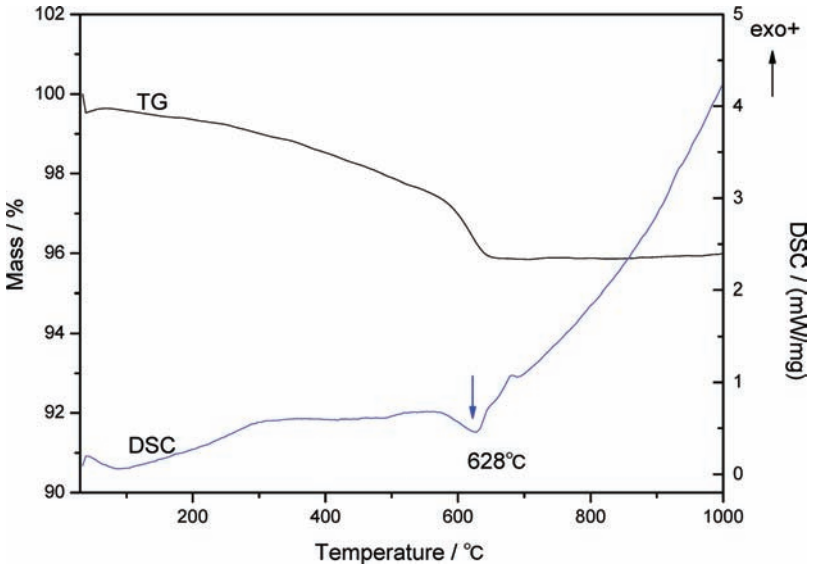

Figure 2. TG-DSC curve of the hydrothermal product hydroxyl sodium yttrium tungstate obtained at 180 °C for 48 h in the presence of P123.

and stirred for 10 min at room temperature. Then solution A was added into solution B, and the mixture was vigorously stirred for about 30 min to ensure that all reagents were dispersed homogeneously. The mixture was transferred into a 25 mL Teflon-lined stainless steel autoclave and filled with deionized water up to a 70% filling capacity of the total volume. The autoclave was sealed and maintained at 180 °C for 1−72 h, and then cooled to room temperature naturally. After the above hydrothermal treatment, the product was centrifuged and washed with deionized water and absolute ethanol several times. And then the precipitate was dried at 70 °C for 24 h and collected for characterization. In addition, we get a portion of the final products for calcination at 630 °C for ~2 h to characterize their structure. For comparison, we systematically carried out a series of experiments by the same hydrothermal process with adjusting the concentration of P123 and the reaction time.

2.3. Characterization. The final products were examined by XRD, TG-DSC, SEM, EDS, TEM, FT-IR, UV−vis spectra, and PL. X-ray powder diffraction (XRD) analyses were carried out on a Bruker D8-Focus X-ray diffractometer with graphite-monochromatized Cu Kα radiation (40 KV/60 mA, graphite monochromator). Thermogravimetric analysis was performed on an STA-409PC/4/H LUXX TG-DSC instrument at a heating rate of 10 K/min to a maximum temperature of 1273 K. The morphology was characterized with a Philips XL-30 environmental scanning electron microscope (ESEM) equipped with an energy-dispersive X-ray spectra (EDS). Transmission electron microscopy (TEM) images were recorded on a JEOL200CX microscope with an accelerating voltage of 200 kV. PL spectra were obtained using a fluorescence spectrophotometer (RF5301) with a xenon lamp as the excitation source. FT-IR data were collected on a Nicolet model 5SXC (America) spectrophotometer in the range of 4000−400 cm^{-1} using KBr pellets. UV−vis diffuse reflectance spectra were recorded on an America BWtek Instantspec BWS003 spectrophotometer equipped with an integrating sphere, using $BaSO_4$ as a reference.

3. Results and Discussion

3.1. Crystal Structure of Hydroxyl Sodium Yttrium Tungstate and $NaY(WO_4)_2$. Figure 1 shows representative XRD patterns of the hydroxyl sodium yttrium tungstate compounds synthesized by a hydrothermal process for 180 °C at different hours (a) 1 h, (b) 3 h, (c) 6 h, (d) 12 h, (e) 24 h, (f) 48 h, (g) 72 h, and (h) $NaY(WO_4)_2$ (prepared by annealing the hydroxyl sodium yttrium tungstate at ~630 °C for 2 h). The products obtained from 1 to 3 h are in the amorphous state because their XRD patterns exhibit a very broad band. It is obvious that by prolonging the hydrothermal reaction time, the crystallization of the hydroxyl sodium yttrium tungstate crystal is improved. Though the diffraction peak of the hydrothermal products became sharper with the longer reaction time, the diffraction peaks can not be indexed to a certain phase because the hydrothermal products may contain some hydrous compounds originating from the water medium. Figure 1 (h) is the XRD pattern of the $NaY(WO_4)_2$ crystals, it can be indexed to JCPDS card of 48-0886 with space group of $I41/a$ [88], and are in agreement with the known tetragonal system. Its unit-cell parameters are $a = b = 5.205$, $c = 11.251$, and it possesses the scheelite structure.[16] No impurity peaks can be detected in Figure 1 (h).

Figure 2 shows the TG-DSC curve of the hydrothermal product. From the TG curve, we can observe that within 30 to 700 °C, there is a ~4% weight loss with an obvious endothermal peak at 628 °C on the DSC curve that corresponds to the loss of coordination hydroxyl in the crystal lattice and a phase transition of forming $NaYW_2O_8$, which is in accordance with XRD analysis.

To better understand the formation process of the hydroxyl sodium yttrium tungstate, we investigate its morphology and PL properties. The influence of various experimental parameters such as the temperature, reaction time, and different concentration of surfactant has been discussed.

The triblock copolymer P123 as the structure directing agent plays a key role in the morphology controlled synthesis.[35] To investigate the influence of P123 on the morphology of the final product, we set a series experiments by hydrothermal method at 180 °C for 48 h in the presence of P123 with different concentrations. As a comparison, the same process is carried out without

(35) Wang, H. N.; Wang, Y. H.; Zhou, X. F.; Zhou, L.; Tang, J. W.; Lei, J.; Yu, C. Z. *Adv. Funct. Mater.* **2007**, *17*, 613.

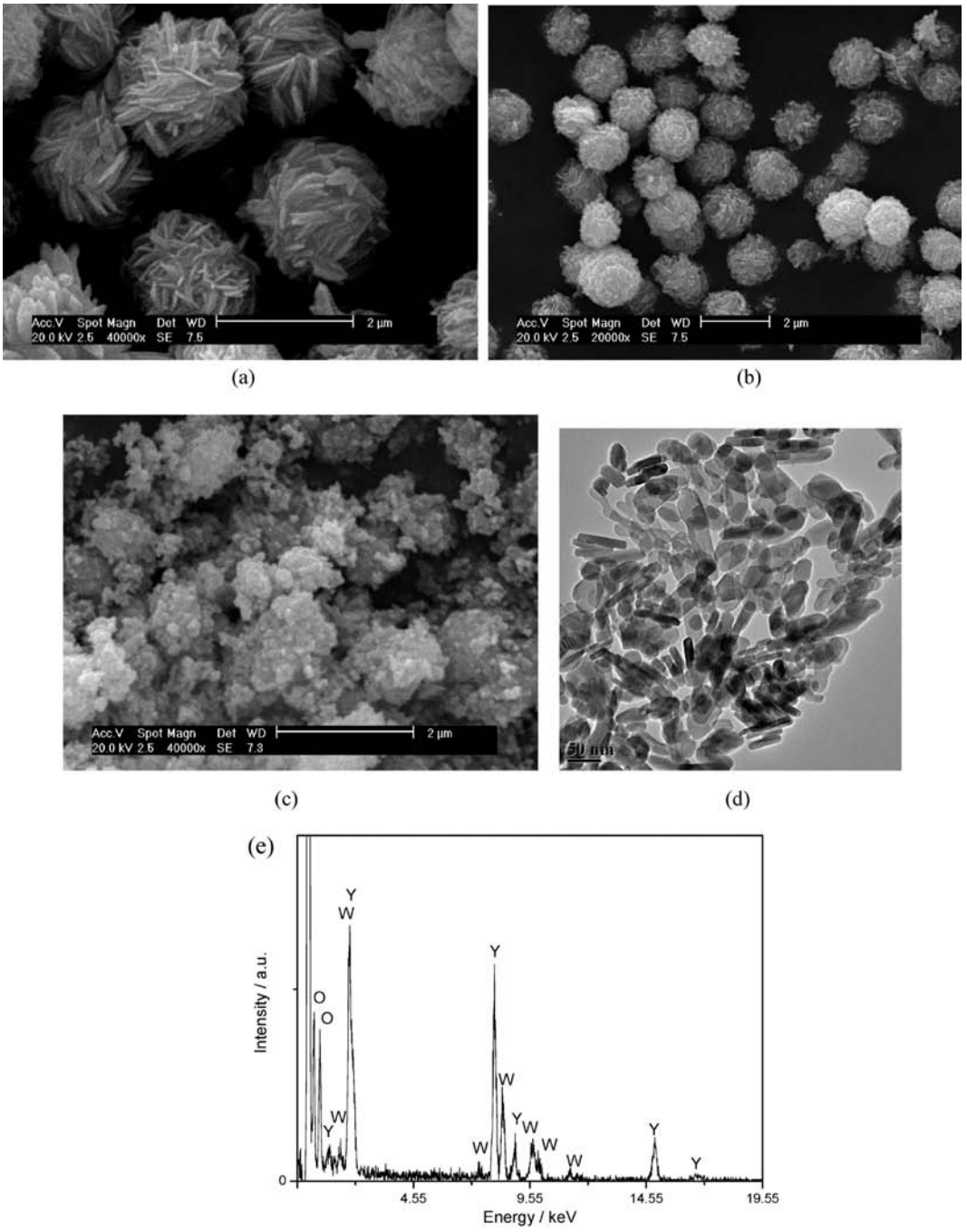

Figure 3. SEM image of (a) hydroxyl sodium yttrium tungstate microspheres obtained by hydrothermal method at 180 °C for 48 h without the presence of surfactant P123, (b) hydrothermal product obtained in the presence of 2.5 g/L P123, (c) hydrothermal product obtained in the presence of 12.5 g/L P123, (d) TEM images of (c), (e) EDS image of (d).

adding P123. Samples obtained without the presence of P123 consist of a high yield of uniform spheroids (Figure 3(a)). The individual microsphere with the diameter of about 1.5 μm is composed of many nanoflakes. The samples obtained in the presence of a certain concentration of P123 (2.5 g/L) with spherical structure are nearly monodisperse (Figure 3(b)), and their average diameter is 1.5−2.0 μm. With increasing the concentration of P123, the morphology of the samples change greatly. When the concentration of P123 increases to 0.0125 g/mL, a great many nanoparticles come into being and seriously agglomerated (Figure 3(c)). That is, as the concentration of the block copolymer increases, fragmentation reactions take over. At a high P123 concentration, the micelles are much longer, causing them to overlap and to form a transient network. Figure 3(d) is the TEM image of these nanoparticles, from the TEM image we can observe that the nanoparticles are elliptical-like particles with the size of ~50 nm. The chemical compositions of a couple of flakes were determined by using EDS. The EDS analysis (Figure 3(e)) shows that the elliptical particles contain Y, W, and O elements, and the molar ratio of Y/W/O is 1:1.22:4. The above results indicate that the concentration of P123 is essential for the formation of

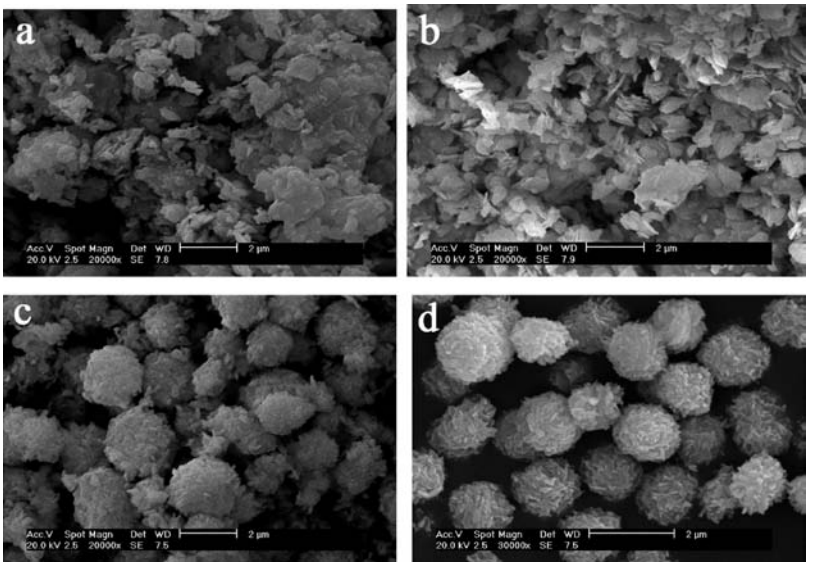

Figure 4. SEM images of the hydrothermal products hydroxyl sodium yttrium tungstate obtained at 180 °C for different time intervals in the presence of 2.5 g/L P123: (a) 1 h, (b) 3 h, (c) 6 h, and (d) 48 h.

hydroxyl sodium yttrium tungstate microspheres, when it increases to 12.5 g/L, the orientation of the spherical micelles have been destroyed.

3.2. Growth Mechanism and Factors Influencing the Formation of Flake-Ball Hydroxyl Sodium Yttrium Tungstate Crystals. The inorganic crystal growth mechanism in solution has caused great attention in recent years because of the interest in size and shape-dependent investigations.[36] Though diversified mechanisms have been carried out, the crystallization process still remains a complicated problem. To clearly understand the growth mechanism of hydroxyl sodium yttrium tungstate multiflake-based spheres, time-dependent shape evolution of the microspheres has been examined. The panels a−d of Figure 4 show the SEM images of the as-prepared hydrothermal products obtained at 180 °C for 1, 3, 6, and 48 h in the presence of 2.5 g/L P123, respectively, they show the time-dependent process of the formation of uniform flake-ball particles from fine amorphous particles. At the initial stage, tiny crystalline nuclei formed incompletely in a supersaturated solution, we can observe large-scale aggregated amorphous particles in Figure 4a. When the hydrothermal reaction is kept for 3 h, large-scale flake-like crystals come into being (Figure 4b), which indicates that the amorphous hydroxyl sodium yttrium tungstate particles tend to aggregate to form flakes after hydrothermal reaction at 180 °C for 3 h. These very thin nanoflakes are responsible for the breadth of the XRD pattern. Prolonging the reaction time for 6 h, flakes begin to self-assemble uniform sphere-like crystals with diameter of ∼1.5 μm (Figure 4c). Minimization of the surface free energy results in the formation of spherical structure particles. The particle size of ∼1.5 μm is almost constant for ∼48 h, and further reaction has little influence on the size of this flake-based sphere, the surface of the spheres are composed of flower-like flakes (Figure 4d). Such anisotropic crystal growth is influenced by the selective adsorption of organic additives P123 on specific sites. Nucleation and growth occur within aggregates of amorphous inorganic particles that are partially stabilized by surface-adsorbed polymers/block copolymers[37] or surfactant molecules.[38,39]

The multiflake-based sphere structure is an interesting hierarchical superstructure. Figure 5(a−e) shows the TEM images of the products obtained by hydrothermal reaction at 180 °C for 48 h in the presence of 2.5 g/L P123 with different morphologies at the same state. Figure 5a shows the low magnification image of the nearly monodisperse spheres. The high magnification image (Figure 5b) exhibits one of the spheres with the diameter of about 1.5−2.0 μm, the sphere is a solid sphere assembled with great many nanoflakes, which can be observed from the edge of the sphere. At the same time, there also coexist other substructures along with the microspheres. Panels c−e of Figure 5 show the TEM image of the substructure crystals with a flower-cluster like morphology. The incomplete growth state can disclose the formation process from nanoflakes to microspheres.

From the above SEM and TEM observations, it can be concluded that the flake-ball microstructures can be obtained via nucleation, crystal growth, and self-assembly growth process. Figure 6 gives a clearly illustration of the formation process of hydroxyl sodium yttrium tungstate polycrystalline flake-ball particles. At the initial stage, the precursor is kept stirring for about 30 min to precipitate completely,and then with hydrothermal treatment for 1 h, the ongoing nucleation process take place, we can observe nuclei deviate from the colloid-like phase. Flake-like crystals formed for about 3 h, this is the growth process of the crystals. With prolonged time, flake-like crystals aggregated and self-assembled into spheres. This self-assembly process from nanoflakes to spheres can be observed clearly by the following three TEM images.

(36) Luo, Z. J.; Li, H. M.; Shu, H. M.; Wang, K.; Xia, J. X.; Yan, Y. S. *Cryst. Growth Des.* **2008**, *8*, 2275.

(37) Yu, S. H.; Cölfen, H. *J. Mater. Chem.* **2004**, *14*, 2124.

(38) Yu, J. G.; Guo, H. T.; Davis, S. A.; Mann, S. *Adv. Funct. Mater.* **2006**, *16*, 2035.

(39) Qi, L.; Ma, J.; Cheng, H.; Zhao, Z. *J. Phys. Chem. B* **1997**, *101*, 3460.

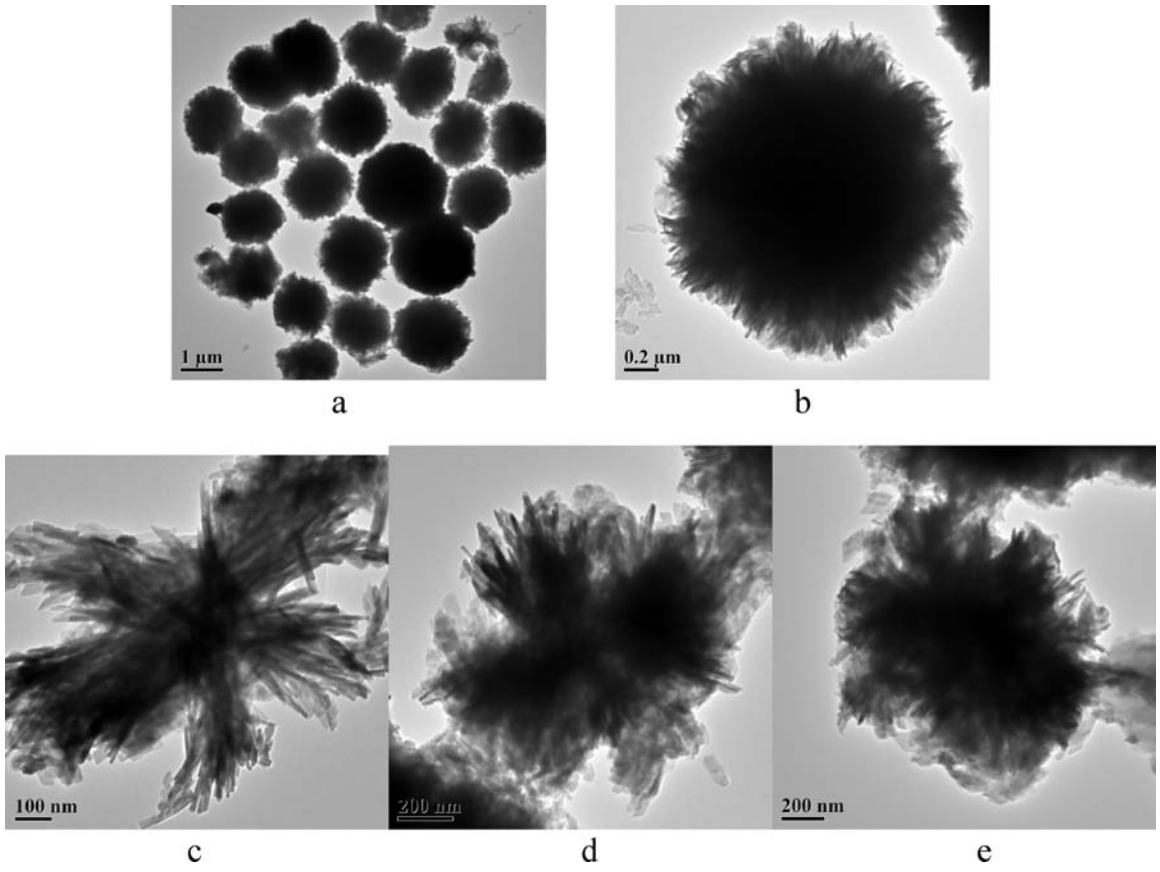

Figure 5. (a−e) TEM images of the hydrothermal products obtained by hydrothermal reaction at 180 °C for 48 h in the prescence of 2.5 g/L P123.

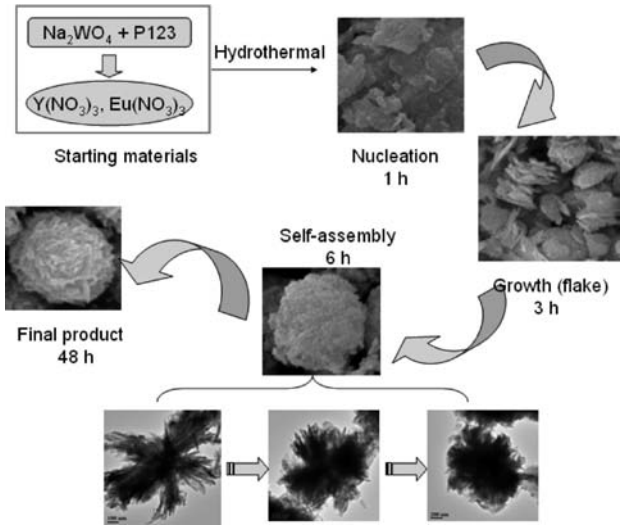

Figure 6. Schematic illustration of the formation process of hydroxyl sodium yttrium tungstate "flake-ball" polycrystalline.

That is, the nanoflakes aggregate to form radiated clusters, then the cluster increases, and finally forms a "flake-ball". When the reaction is kept for certain hours we can obtain the "flake-ball" with a flower-like surface. So we believe the hydroxyl sodium yttrium tungstate growth process is the self-assembly process under the influence of the triblock copolymer.

The interaction between $NaY(WO_4)_2$ and the hydrothermal products hydroxyl sodium yttrium tungstate with or without the presence of P123 is investigated by the FT-IR spectra. Figure 7 shows the FT-IR spectra of the hydrothermal products (a) without the presence of P123, (b) with the presence of 25 g/L P123, and (c) the hydrothermal product with heat treatment at 630 °C for 2 h ($NaY(WO_4)_2$). There are broad bands at 3445 and 1638 cm^{-1} in the (a) to (c) spectra, corresponding to the surface-absorbed water and hydroxyl groups, respectively. The sharp band peaking at 3559 cm^{-1} (Figure 6a,b) is attributed to the O−H vibration of the coordination water. In Figure 7c, there is no existence of 3559 cm^{-1}, which means that the O−H groups have been removed by the heat treatment at 630 °C. The band at ∼2360 cm^{-1} comes from a small quantity of CO_2 in the air. The band at 965 cm^{-1} is assigned to the W=O stretching vibration.[40] The $NaY(WO_4)_2$ compound with sheelite structure has the similar vibration mode as $CaWO_4$.[41] The vibration band at 831 cm^{-1} is assigned to W−O stretching vibration (Figure 6c). There is not much difference from the FT-IR spectra of hydrothermal products with or without the presence of P123. The band range from 450 to 700 cm^{-1} confirms that the tungstate ions in this structure are not additionally connected to each other by intermolecular interactions forming oxygen bridges.

3.3. PL Properties of the As-Prepared Products. It is important to investigate the optical properties of the novel Eu^{3+}-doped hydroxyl sodium yttrium tungstate and $NaY(WO_4)_2$ flower-like spheres. UV−visible diffuse reflectance spectrum (DRS) characterization is employed

(40) Wang, Z. X.; Zhou, S. X.; Wu, L. M. *Adv. Funct. Mater.* **2007**, *17*, 1790.
(41) Lei, F.; Yan, B. *J. Solid State Chem.* **2008**, *181*, 855.

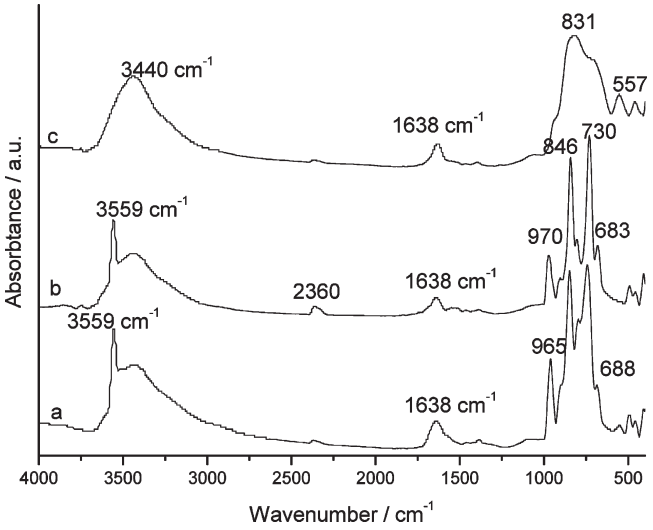

Figure 7. FT-IR spectra of the hydrothermal products (a) without the presence of P123, (b) 25 g/L P123 and (c) $NaY(WO_4)_2$.

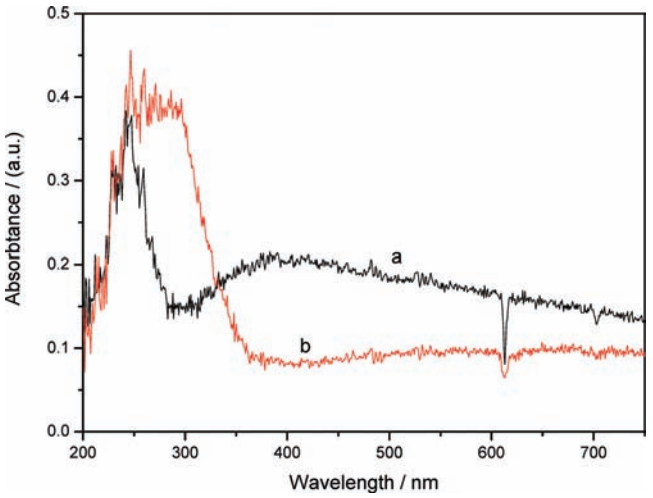

Figure 8. UV−vis spectra of the (a) hydrothermal product hydroxyl sodium yttrium tungstate and (b) $NaY(WO_4)_2$.

to measure the absorption spectrum. Figure 8 shows the typical absorption spectra of (a) hydroxyl sodium yttrium tungstate and (b) $NaY(WO_4)_2$. The wavelength at the absorption edge, λ, was determined as the intercept on the wavelength axis for a tangential line drawn on the absorption spectra. The optical band gap (Eg) can be estimated by the equation: $Eg = 1240/\lambda(\text{nm})$. On the basis of the DRS absorbance, estimation of the optical band gap (Eg) is 3.88 eV for hydroxyl sodium yttrium tungstate, and 3.2 eV for $NaY(WO_4)_2$. The obvious shift in the absorption edge is assigned to the distorted WO_4^{2-} groups in the hydrothermal product of hydroxyl sodium yttrium tungstate. The spectrum of $NaY(WO_4)_2$ has a broadband ranging from 200 to 370 nm, which is owed to the O−W CT transition. Compared with $NaY(WO_4)_2$, the hydrothermal product has a relative narrow O−W CT transition band range from 200 to 280 nm. The downward peak at 613 nm is assigned to the Eu^{3+} doped in the hosts.

We investigate the PL studies of the Eu^{3+} doped hydrothermal product hydroxyl sodium yttrium tungstate and $NaY(WO_4)_2$ in the range of 300−750 nm at room temperature. The excitation spectra are obtained by

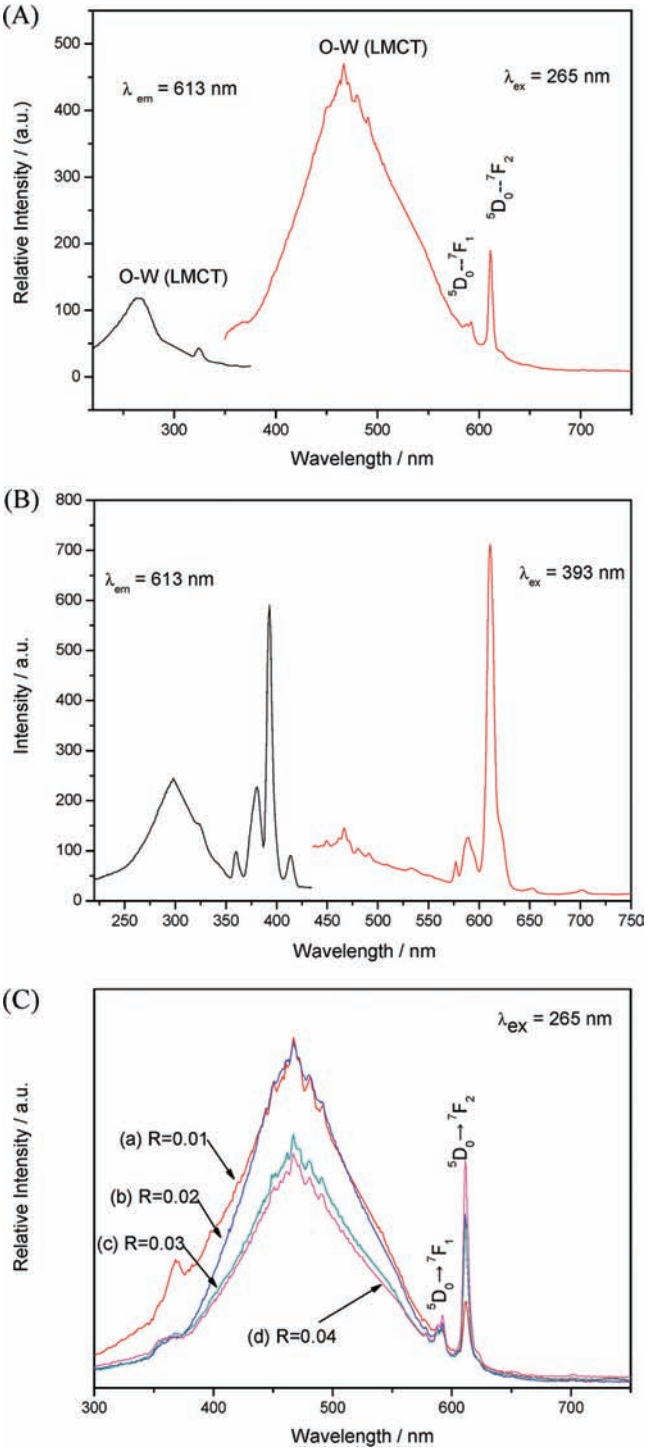

Figure 9. Excitation and emission spectra of Eu^{3+} doped (a) hydroxyl sodium yttrium tungstate and (b) $NaY(WO_4)_2$ (c) Emission spectra of Eu^{3+} doped hydroxyl sodium yttrium tungstate phosphor with different molar ratio R (Eu^{3+}/Y^{3+}): (a) $R = 0.01$, (b) $R = 0.02$, (c) $R = 0.03$ and (d) $R = 0.04$.

monitoring the $^5D_0 \rightarrow {}^7F_2$ transition of Eu^{3+} at 613 nm. Figure 9A shows the excitation and emission spectra of the hydrothermal product hydroxyl sodium yttrium tungstate, the excitation spectrum shows a broad CT (O→W) band ranging from 220 to 300 nm. The emission spectrum is taken under the excitation wavelength at 265 nm, which contains two parts: one is the strong broadband of ligand to metal CT (LMCT) transition of (O→W), the

other sharp lines are the characteristic transition of Eu^{3+} at ~592 and ~611 nm, which corresponds to the magnetic dipole transition ($^5D_0 \rightarrow {}^7F_1$) and electric dipole transition ($^5D_0 \rightarrow {}^7F_2$), respectively.

While for $NaY(WO_4)_2$ (Figure 9B), there are some differences from the PL spectra of hydroxyl sodium yttrium tungstate. The excitation spectrum shows a broad CT (O→W) band range from 220 to 350 nm, peaking at 298 nm along with sharp lines of Eu^{3+} at ~359, ~380, ~393, and ~413 nm. The broadband is ascribed to the ligand to metal CT transition (LMCT) $O^{2-} \rightarrow W^{6+}$ of WO_4^{2-} group, and the sharp lines correspond to the Eu^{3+} transitions of $^7F_0 \rightarrow {}^5D_4$, $^7F_0 \rightarrow {}^5L_7$, $^7F_0 \rightarrow {}^5L_6$, and $^7F_0 \rightarrow {}^5D_2$, respectively. Among the sharp lines, the most intense band is at 393 nm. The emission spectrum exhibits the strongest sensitized luminescence from Eu^{3+} when excited at 393 nm, it is composed of a weak broadband and the sharp lines of $^5D_0 \rightarrow {}^7F_J$ transitions ($J = 0, 1, 2, 3, 4$) of Eu^{3+} at ~577, ~588 and ~611, ~651, and ~701 nm, respectively. Usually, the luminescence intensity ratio of electric dipole transition and magnetic dipole transition is regarded as a probe to detect the inversion environmental symmetry around Eu^{3+} in the host. The $^5D_0 \rightarrow {}^7F_2$ intensity is about six times more than that of the $^5D_0 \rightarrow {}^7F_1$ transition. The dominance of electric dipole transition implies the Eu^{3+} is located at a site of non-inversion symmetry.[42,43]

Different molar ratios R of Eu^{3+}/Y^{3+} have a great influence of color diversity of Eu^{3+} doped hydroxyl sodium yttrium tungstate phosphor. As discussed in Figure 9A, we know that the spectrum of this phosphor is composed of the green-blue band and the orange-red band, so by adjusting the molar ratio R of Eu^{3+}/Y^{3+}, we can obtain the white light. Figure 9C shows the emission spectra of Eu^{3+} doped hydroxyl sodium yttrium tungstate phosphor with different molar ratio R (Eu^{3+}/Y^{3+}), (a) $R = 0.01$, (b) $R = 0.02$, (c) $R = 0.03$, and (d) $R = 0.04$. Through the experiments, we find when $R = 0.02$, the phosphor emits white light under the UV excitation. That is to say, by adjusting the ratio of the green-blue band and orange-red band to a certain value, we can obtain white-light emission phosphor, which is different from the white-light phosphor that Huang et al. had reported.[24]

We also examine the PL variation with different morphologies influenced by reaction time. Figure 10A (a) to (g) shows the emission spectra of hydroxyl sodium yttrium tungstate at different reaction time ((a) 1 h, (b) 3 h, (c) 6 h, (d) 12 h, (e) 24 h, (f) 48 h, and (g) 72 h). Except for the relative intensity, there is not much difference from these emission spectra. All of the spectra contain a broad O−W (CT) transition and the characteristic transition of Eu^{3+} at ~592 and ~611 nm. Theoretically, the PL intensity increases with prolonged reaction time because the longer the reaction interval, the better crystallization and the luminescent properties. From the experiments data, we can conclude that for hydroxyl sodium yttrium tungstate crystals, the PL properties have not changed by the morphologies from nanoflakes to spheres, for the spheres are self-assembled by the nanoflakes and the type of the force belongs to van der Waals force.

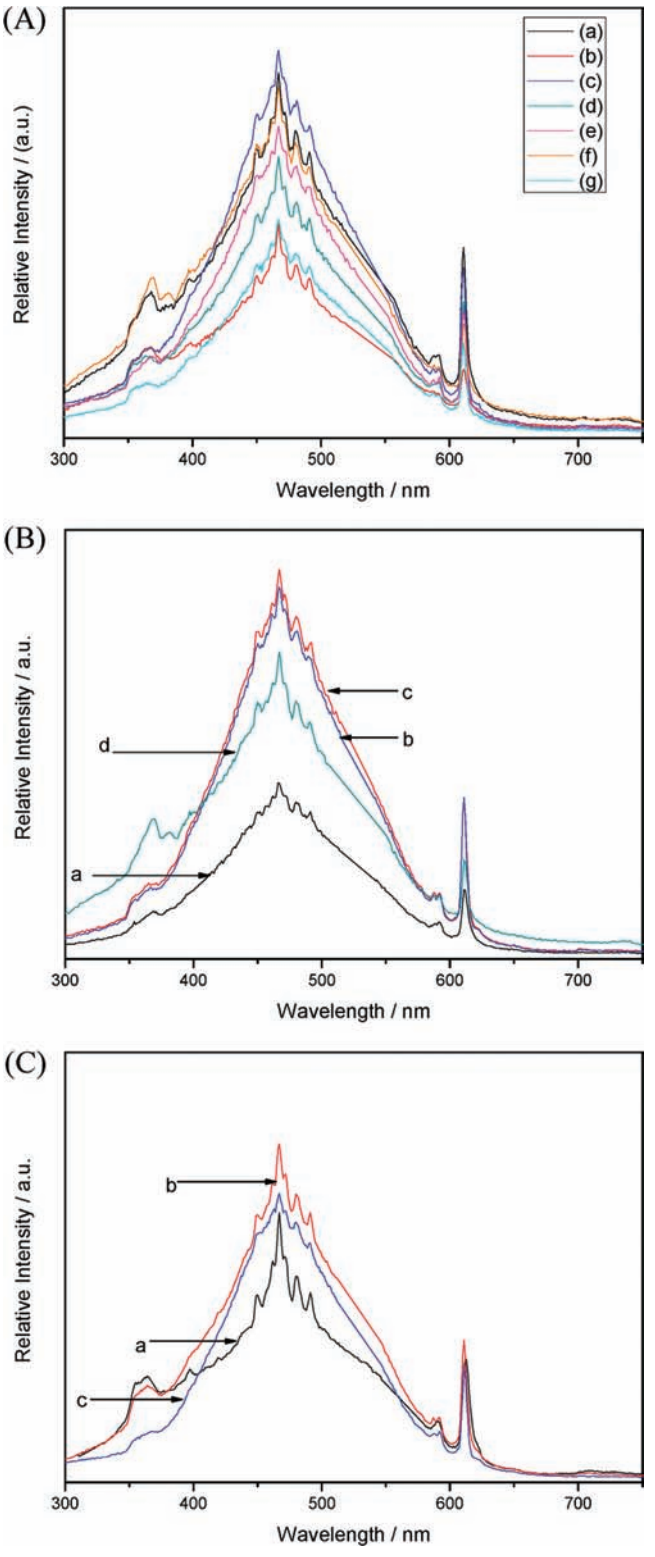

Figure 10. (A) Emission spectra of the products obtained by hydrothermal synthesis at 180 °C for different reaction time (a) 1 h, (b) 3 h, (c) 6 h, (d) 12 h, (e) 24 h, (f) 48 h, and (g) 72 h. (B) Emission spectra of hydroxyl sodium yttrium tungstate obtained by hydrothermal synthesis in the presence of different concentration of P123 (a) 0 g, (b) 2.5 g/L, (c) 12.5 g/L and (d) 25 g/L. (C) Emission spectra of the product synthesized by hydrothermal method at different temperatures (a) 120 °C, (b) 150 °C, and (c) 180 °C for 24 h.

(42) Ozawa, T. C.; Fukuda, K.; Akatsuka, K.; Ebina, Y.; Sasaki, T. *Chem. Mater.* **2007**, *19*, 6575.
(43) Wang, Y.; Gao, H. *J. Solid State Chem.* **2006**, *179*, 1870.

The different concentration of P123 has some influence on the PL intensity. Figure 10(B) (a) to (d) shows the emission spectra of hydroxyl sodium yttrium tungstate obtained by hydrothermal process in the presence of different concentration of P123 (a) 0 g, (b) 2.5 g/L, (c) 12.5 g/L, and (d) 25 g/L. P123 form micelles in aqueous solution, the formation of P123 micelles is due to the differential solubility of EO and PO units in water. As Alexandridis et al. has reported, the critical micellar concentration of P123 is 2 g/L (20 °C).[44] At low surfactant concertration, single chain entry/exit is the major driving force, but as the concentration of the block copolymer increases, fragmentation reactions take over.[45] As discussed before, the concentration of P123 plays a key role in the morphology of the final products. When the concentration of P123 over its CMC, fragmentation processes take place. The PL intensity of the sample obtained without adding any P123 is the lowest. The PL intensity of the samples obtained in the presence of 2.5 g/L and 12.5 g/L is increased distinctively. However, when the P123 concentration reaches 25 g/L, the PL intensity decreases. The results indicate that adding P123 is good for PL properties, while adding additional amounts of P123 will damage the PL intensity.

The influence of hydrothermal temperature on the PL intensity is also investigated. We set a series experiments to investigate the PL intensity of the samples obtained by hydrothermal process at different temperatures of 120, 150, and 180 °C for 24 h. As can be seen from Figure 10C, the spectrum of the as-prepared product obtained at 120 °C has a relative low PL intensity of the broadband range from 300 to 600 nm. With the temperature increasing, the intensity of the CT transition increased too, which agrees with the XRD pattern, namely, the higher the temperature, the better the crystallization.

(44) Alexandridis, P.; Holzwarth, J. F.; Hatton, T. A. *Macromolecules* **1994**, *27*, 2414.

(45) Denkova, A. G.; Mendes, E.; Coppens, M. O. *J. Phys. Chem. B.* **2009**, *113*, 989.

4. Conclusion

Large-scale three-dimensional micrometer-sized spherical polycrystalline Eu^{3+} doped white light hydroxyl sodium yttrium tungstate monodisperse "flake-ball" microarchitectures are prepared by a well-known hydrothermal approach at 180 °C for 48 h in the presence of triblock copolymer P123. Eu^{3+} doped $NaY(WO_4)_2$ phosphor with scheelite structure was obtained by annealing hydroxyl sodium yttrium tungstate crystals at ~630 °C for 2 h. When the molar ratio R of Eu^{3+}/Y^{3+} reached 0.02, the hydrothermal product is a potential white light material under UV excitation. The crystal growth process of the hydrothermal product is dominated by the self-assembly process of triblock copolymer P123. Morphology controlled synthesis of the nanoflake spheres has been readily achieved by changing the experimental parameters. We can obtain the flakes assembled microspheres at a moderate P123 concentration less than 12.5 g/L by the hydrothermal process at 180 °C for ~48 h. The excitation spectrum of Eu^{3+} doped white light phosphor hydroxyl sodium yttrium tungstate shows a broad CT (O → W) band ranging from 220 to 300 nm. Its emission spectrum contains two parts: one is the strong broadband of ligand to metal CT (LMCT) transition of (O→W), the other has the sharp lines of Eu^{3+} at ~592 ($^5D_0 \rightarrow {}^7F_1$) and ~611 nm ($^5D_0 \rightarrow {}^7F_2$), respectively. The emission spectrum of Eu^{3+} doped $NaY(WO_4)_2$ phosphor exhibits the strongest sensitized luminescence from Eu^{3+} when excited at 393 nm, it was composed of a weak broadband and the sharp lines of $^5D_0 \rightarrow {}^7F_J$ transitions (J = 0, 1, 2, 3, 4) of Eu^{3+} at 577, 588, 611, 651, and 701 nm, respectively. The $^5D_0 \rightarrow {}^7F_2$ intensity is about six times more than that of the $^5D_0 \rightarrow {}^7F_1$ transition. The dominance of electric dipole transition implies the Eu^{3+} is located at a site of non-inversion symmetry in $NaY(WO_4)_2$ crystal.

Acknowledgment. The authors gratefully acknowledge the financial support from the National Science Foundation of China (No. 20671072) and Program for New Century Excellent Talents in University (NCET-08-0398).